Alexandria Engineering Journal (2016) xxx, xxx–xxx

HOSTED BY

Alexandria University

Alexandria Engineering Journal

www.elsevier.com/locate/aej
www.sciencedirect.com

ORIGINAL ARTICLE

Influence of aspect ratio on the thermal performance of rectangular shaped micro channel heat sink using CFD code

D.R.S. Raghuraman [a], R. Thundil Karuppa Raj [a,*], P.K. Nagarajan [b], B.V.A. Rao [a]

[a] School of Mechanical Engineering, VIT University, Vellore 632 014, Tamil Nadu, India
[b] Department of Mechanical Engineering, S.A. College of Engineering, Chennai, Tamil Nadu, India

Received 27 June 2016; revised 5 August 2016; accepted 29 August 2016

KEYWORDS

Micro channel heat sinks (MCHS);
Aspect ratio (AR);
Reynolds number;
Nusselt number friction factor;
CFD

Abstract A numerical study has been carried out to investigate the heat transfer enhancement and fluid flow characteristics for various aspect ratios of rectangular micro channel heat sinks (MCHS). The working fluid considered for the analysis is water. The fluid flow and heat transfer characteristics of a three-dimensional MCHS are obtained numerically by solving the appropriate governing equations. The flow domain is discretized as finite volume elements and solved using ANSYS CFX 14.5, commercially available CFD code. The numerically predicted results obtained through CFD code are validated with the experiments carried out and it is found that the maximum deviation between the two is less than 5%. Hence the CFD code is further extended to study the influence of geometrical parameters. The channel size optimization has been carried out numerically to obtain the effective heat removal from the MCHS. Average convective heat transfer coefficient, outlet temperature, friction and pressure drop, pumping power and thermal resistance have been plotted against Reynolds number. Non-dimensional parameter, Nusselt number has been plotted as a function of Reynolds number for three heat sinks with different aspect ratios. Friction factor and pressure drop across the channels are obtained and plotted across the channels.

1. Introduction

Technology involving high speeds of data processing in microprocessors of fast computers has led to reduction in sizes of integrated chips. The need to remove large amount of heat generated from such devices for effective functional characteristics was first investigated by Tuckerman and Pease [1]. In their work, they had studied the experimental and theoretical performance of micro channels as heat exchangers using water as the coolant and suggested the use of high aspect ratio micro channels to reduce thermal resistance.

Steinke and Kandlikar [2] in their review article, had summarized the various efforts made by researchers across the globe, on single phase heat transfer in the micro channels. They investigated the influence of various parameters such as Nusselt number, Reynolds number, heat transfer coefficient, thermal resistance and friction factor, with respect to fluid flow

* Corresponding author.
E-mail address: thundilr@gmail.com (R. Thundil Karuppa Raj).
Peer review under responsibility of Faculty of Engineering, Alexandria University.

http://dx.doi.org/10.1016/j.aej.2016.08.033

Nomenclature

A	cross-sectional area (m^2)
A_{eff}	effective cross-sectional area (m^2)
AC	Alternate Current (amps)
AR	aspect ratio
c_p	specific heat capacity of water (J/kg K)
CFD	Computational Fluid Dynamics
D_h	hydraulic diameter (m)
f	friction factor
h_{avg}	average wall heat transfer co-efficient (W/m^2 K)
H	micro channel height (m)
H_g	mercury
k	thermal conductivity (W/m K)
L	micro channel length (m)
m	mass flow rate of water (kg/s)
MCHS	micro channel heat sink
n	number of channels
N_u	Nusselt number
P	perimeter (m)
P_c	Poiseuille constant
Q	heat released (W)
Q_b	heat flux at the bottom surface (W/m^2)
R_e	Reynolds number
T	base and top thickness (m)
T_{in}	inlet temperature (K)
T_{out}	outlet temperature (K)
TR	thermal resistance (°C/kW)
T_w	wall temperature (K)
T_{wmax}	maximum wall temperature (K)
U_m	inlet mean velocity (m/s)
V	volumetric flow rate (m^3/s)
VARIAC	VARIABLE RHEOSTAT
W_c	micro channel width (m)
W_w	micro channel wall width (m)
W_{pp}	pumping power (W)
∇P	pressure drop (Pa)
ρ	density (kg/m^3)
μ	dynamic viscosity of water (Ns/m^2)

and heat transfer characteristics by their experimental studies. They had also discussed about enhanced micro channel heat sinks, where very high heat fluxes of 500 W/cm^2 have to be removed for the proper operation of the micro channel heat sinks. Rathanasamy and Kalaivanan [3] had conducted experiments related to forced convection through rectangular micro channels. The channels were selected in two batches, one having 47 micro channels with hydraulic diameter of 387 μm each, and the second one having 50 micro channels with hydraulic diameter of 327 μm each. The channels were fabricated on stainless steel substrate. Their study involved ethanol, methanol and ethanol–methanol mixture as working fluid under laminar flow regime. Flow parameters such as flow rate and velocity were monitored and recorded along with temperature profile along the length of the channels. The measured temperature distribution was used to obtain the average Nusselt number and heat transfer characteristics. Iyengar and Garimella [4] had carried out both analytical and experimental studies on copper micro channel heat sinks using water as the coolant. The analytical design has helped in optimizing the flow geometry for enhancing the heat transfer by 24% in the MCHS.

Wong and Ghazali [5] had simulated a CFD model of a micro channel heat sink to study fluid flow and heat transfer phenomena across the MCHS. The channels in their analytical work were rectangular and made from silicon. They have analyzed the model for flows up to Reynolds number of 400. They obtained temperature and heat flux distribution along the channel length. Ellsworth et al. [6] in their review paper had discussed the high end cooling technology for high speed IBM servers. These, though not at the micro level, still generate a large amount of heat and require secondary cooling system and the authors had adopted a dual coolant technology (air-to-water cooling) for effective heat removal.

Qu et al. [7] carried out experimental and numerical studies on heat transfer and fluid flow through trapezoidal micro channels and compared the predicted numerical results with their experimental work. The hydraulic diameters of the silicon micro channels were in the range from 62 to 169 μm. Nusselt numbers obtained in experiments were lower than the analytical results. This may be due to the rough surfaces of the MCHS which has not been considered in the numerical analysis. The above study had indicated the importance of surface roughness in influencing the heat transfer characteristics across the MCHS. Naphon and Khonseur [8] had studied the pressure drop and heat transfer characteristics along a micro channel heat sink for constant heat flux operating condition. They had examined the heat transfer characteristics by varying the length and width of the micro-channel and reported that the channel dimension had played a crucial role in the heat transfer characteristics and performance of the micro-channel heat sink.

Yu and Ameel [9] had presented the heat transfer studies in a rectangular flow channel using gas as the cooling medium and found that the effects of expansion of the gas resulted in a heat transfer loss up to 40%. They reported that higher surface to volume ratio of heat sinks, and low pumping power characterizes the micro channels as good heat exchangers.

Khan et al. [10] had carried out numerical simulations on 2-dimensional and 3-dimensional micro channel heat sinks and plotted the temperature distributions along its length. They used nitrogen and hydrogen as the working fluid and had found that hydrogen has better heat transfer characteristics compared to nitrogen. Khamaneh et al. [11] had studied micro channel heat sink under forced convection and for laminar flow condition. The investigators had performed numerical as well as experimental work on rectangular micro channels, with water as the coolant. They had concluded that with increasing Reynolds number, pressure drop also increases. Also, they found that, geometric changes such as increase in width of the MCHS, decrease in height of the micro channels, and increase in the hydraulic diameter greatly influence the average Nusselt number and heat transfer characteristics.

Raghuraman et al. [12] had carried out experiments on rectangular high aspect ratio copper micro channel heat sink using

Please cite this article in press as: D.R.S. Raghuraman et al., Influence of aspect ratio on the thermal performance of rectangular shaped micro channel heat sink using CFD code, Alexandria Eng. J. (2016), http://dx.doi.org/10.1016/j.aej.2016.08.033

TiO_2 nano fluid as the working fluid and they had investigated the thermal and fluid flow characteristics across the MCHS. The fluid flow and thermal performance of 0.1% and 0.3% nano powder suspensions in water were compared with the parent fluid, water. It was found that 0.3% volume fraction nano fluid exhibited better performance than 0.1% volume fraction nano fluid. Amanifard and Haghi [13] had performed numerical studies on three dimensional rectangular micro channel heat sinks and studied the effects of flow rate and channel geometry on the heat dissipation capability and pressure drop of the systems. Qu and Mudawar [14] had carried out experiments and numerically simulated the pressure drop and heat transfer characteristics of a single phase micro channel heat sink and they demonstrated that the conventional Navier-Stokes and energy equation could adequately predict the fluid flow and heat transfer characteristics of the micro channel heat sinks. Mishan et al. [15] had used infrared technique to design and built a micro channel test section that could measure the local and average Nusselt numbers with bulk fluid temperature.

The heat produced in the integrated circuits should be effectively removed and the temperature should be maintained below a particular value in order for the electronic systems to function properly and with better life span. In this regard, Hassan et al. [16] had made an state-of-the-art literature review on the microchannel heat sinks developed for removing the heat produced in the integrated circuits. They had briefly explained about various progresses of removing the heat generated in the integrated circuits over a decade. The effect of circular, square and trapezoidal grooved tubes in the heat transfer characteristics was analyzed numerically with the help of computational fluid dynamics code and the results were compared with the plain tube by Selvaraj et al. [17] and they reported the analysis can be extended to micro channel heat sinks also. Zhang et al. [18] had reported from their studies that the micro channel heat sink with liquid metal possesses relatively lower thermal resistance compared to water as working fluid. Thus they reported that liquid metals may be an alternate source for water with better heat transfer characteristics but with slightly higher pressure drop across the channel. Salimpour et al. [19] had studied the effect of non-circular shapes in the optimization of heat transfer characteristics of micro channel heat sinks. They have analyzed the rectangular, elliptic and isosceles triangular cross sections of the micro channel heat sinks and found that both rectangular and elliptical micro channel heat sinks have similar performance and the isosceles triangle MCHS had shown weaker performance. Dharaiya and Kandlikar [20] had developed correlations for Nusselt number for heat transfer in rectangular micro channels for both developing and fully developed laminar flows and this technique was very much useful for the design and optimization of micro channel heat sinks and other microfluidic devices. Xie et al. [21] had carried out numerical study in the mini channel heat sinks to study the heat transfer characteristics for laminar flow. They had optimized the geometry using water as the working fluid for effective heat dissipation and lesser pressure drop. Xie et al. [22] had numerically analyzed the influence of bifurcations on the thermal performance of micro channel heat sinks using CFD code. They had designed five various types of MCHS with bifurcation and one plane MCHS without bifurcation. They examined and reported that the bifurcation model gives better heat transfer characteristics with optimal pressure drop compared to the plane one and they also suggested that the maximum number of bifurcation should be limited to two. Hung et al. [23] had investigated the effect of different configurations of porous micro channel heat sinks on their thermal performance. They had analyzed six various configurations of porous heat sinks and ended up with sandwich configuration which yielded better thermal performance. They mainly concluded that the porous micro channel heat sinks need not be efficient over the non-porous micro channel heat sinks at low pumping power. Lin et al. [24] had studied the effect of double layer micro channel heat sink and their thermal performance numerically for a three dimensional geometry. The working fluid was water and they had examined six different types of double layer heat sinks. They had optimized the dimension of the double layer heat sink for a particular volumetric flow rate and pumping power and they had reported that the double layer heat sink should be examined for every particular application as it varies for different working conditions and could not be generalized.

Xie et al. [25] had studied recently about the obstruction induced in the path of the micro channel heat sink. They reported that the boundary layers get destroyed and new boundary layers have been built which aid in the thermal performance of the heat sinks. They evaluated that obstruction length plays a dominant role in thermal performance of the MCHS. Latest researches are going on, in investigating the effect of magnetic influence, porous medium and nanoparticles in enhancing the heat transfer characteristics of liquid coolants used for various applications including MCHS and have been briefly discussed as follows. Sheikholeslami et al. [26] had carried out an intensive research on the influence of magnetic field on the copper oxide water nano fluid flow and heat transfer characteristics using Lattice Boltzmann method. Koo–Klein streuer–Li correlation was employed to calculate the thermal conductivity and viscosity of the working fluid. They concluded that the heat transfer characteristics increases with increase in Hartmann number and heat source length and decreases with Rayleigh number. Zeeshan et al. [27] had worked on water and ethylene glycol based nanofluid heat transfer characteristics with an inverted cone, by varying the wall temperature and predicted the natural convective boundary layer flow and magnetic effect using nonlinear ordinary differential equation employing Boussinesq approximation. They derived a correlation for skin friction and heat transfer rate for the above model which incorporates porous medium also. Zeeshan and Majeed [28] has critically examined the Non-Darcy boundary layer flow of non-conducting real fluid. The analysis was carried with magnetic ferro particles over a permeable linearly stretching surface taking into account the Ohmic dissipation along with mixed convective heat transfer. They converted the existing governing partial differential equations into nonlinear ordinary differential equations by similarity transformation. They concluded that the skin friction coefficient increases and Nusselt number decreases with increase in ferro magnetic interaction parameter.

The influence of radiation effect and heat transfer characteristics of a ferro-magnetic fluid flow over a stretched sheet was investigated recently by Zeeshan et al. [29]. They established the influence of magnetic dipole and thermal radiation on various non-dimensional parameters such as skin friction and Nusselt number. Ellahi et al. [30] had recently analyzed the impact of shapes of nano-fluid on entropy generation by

Please cite this article in press as: D.R.S. Raghuraman et al., Influence of aspect ratio on the thermal performance of rectangular shaped micro channel heat sink using CFD code, Alexandria Eng. J. (2016), http://dx.doi.org/10.1016/j.aej.2016.08.033

developing a mathematical model analytically using Boussinesq approximation. They investigated the natural convection boundary layer flow over an inverted cone by considering simultaneously the power law effects, porous medium, magnetohydrodynamics and radiation effects in their study. The influence of various parameters such as Rayleigh number, Prandtl number, power law and magnetic effect with porosity index is studied and corresponding Nusselt number and skin friction coefficients have been obtained and reported.

From the literature review surveyed, it is obvious that a number of studies both numerically and experimentally have been carried out to improve the heat transfer characteristics of the micro channel heat sinks. The current study also aims to investigate the thermal performance of rectangular micro channel heat sinks with varying aspect ratios. As seen from the literature cited above, the dimensions of the micro channel play a vital role in the heat transfer characteristics and effective heat removed with optimum pumping power. In this numerical research work, the effect of height to width ratio for three different cases is analyzed numerically and the various output characteristics such as outlet temperature, pressure drop across the channel, heat removed, pumping power required, friction factor, Poiseuille's constant and thermal resistance are plotted for various Reynolds number ranging from 50 to 350 in steps of 50. Thus a most elaborative study on the thermal performance of the micro channel heat sinks with respect to the above parameters is discussed and presented.

2. Experimental setup

The micro channel heat sink using copper is fabricated with overall dimensions of 36.75 width, 31 mm length and 122 channels for carrying out the experimental work. The width of the wall (W_w) between the channels is 150 μm and the width of the channel is also made to 150 μm with a height (H) of 7 mm using electron discharge machining process. The geometry of the micro channel is shown in Fig. 1 and the dimensions of the MCHS are tabulated in Table 1.

The schematic sketch of the experimental setup is shown in Fig. 2. The experimental set up consists of a heat exchanger (MCHS) assembly, a circulating pump to circulate the coolant (De-ionized water), the coolant filter, a flow meter to measure the volumetric flow rate and a control valve to vary the flow rate of the coolant at a prescribed value. A reservoir tank is provided before the circulating pump to collect and store the coolant exiting from the micro channel heat sinks. The coolant from the reservoir tank is pumped to an air cooled fan, by a circulating pump, and thereby the temperature of the coolant is brought down to room temperature. The pump used is a centrifugal pump capable of delivering high flows up to 350 lpm with a maximum head of 4.5 m. But the pump flow to the MCHS is reduced to match the flows ranging from 1 to 3 lpm using a flow control valve. The cooler possesses a secondary fan which cools the exiting coolant by convection. A pictorial representation of the experimental setup is shown in Fig. 3 for more clarity.

The source of heat is provided at the bottom surface of the micro channel heat sink. The heater is of plate type made of ceramic material with a maximum heat input of 900 W/230 V. An electrical heater is used as a source of input heat to the MCHS, which can be changed with the help of a VARIAC. The instruments used for measuring the electrical power are a voltmeter and an ammeter. The AC voltage from the main power supply is decreased using a step–down transformer so that the heat input to the bottom surface of the micro channel heat sink is maintained around 100 W.

In order to measure the wall surface temperatures, four thermocouples are placed strategically at the channel and the heater interface. The average bulk wall temperature is measured using K-type thermocouples with 1 mm diameter beads. The temperature measurements of the liquid coolant are made using two additional thermocouples spaced 2 cm close to the inlet as well as the outlet of the channel. The pressure drop across the MCHS is measured using a U tube manometer which uses mercury and has a resolution of 1 mm of Hg. Since the flow rates occur between 1 and 3 lpm, a flow meter that can measure such low flows but with a maximum rating of 50 lpm is used. The flow control valve and flow meter are located near the return line of the liquid from the micro channel.

The layout of the experimental work is indicated in Fig. 2. A photograph of the experimental setup is shown in Fig. 3. Ceramic based compound is applied at the heater and channel sink interface to avoid air gaps and ensure effective transfer of heat. Also the channel with heater assembly is insulated using glass wool to minimize heat losses.

3. CFD analysis

3.1. Geometric modeling

The modeling of the micro channel has been carried out as a three layer model with the central layer simulating the coolant flow and the side layers representing the solid channel walls. The micro channel with a width of 150 μm and a height of 7000 μm corresponding to an aspect ratio of 46.66 and a length of 31 mm is modeled in ICEMCFD software. The solid channel wall of 75 μm is considered on both sides of the coolant flow.

The 3-dimensional heat sink model is checked for consistency and free of surface errors before meshing.

The fluid flow and heat transfer simulations have been carried out using commercial CFD tool, ANSYS CFX 14.5. The coolant used in the experiments is water and the same is used in CFD studies for validation and parametric studies. A single phase laminar fluid flow and heat transfer analysis is carried out. Continuum flow is assumed inside the micro heat exchanger. The flow field and heat transfer characteristics through the micro channel heat sink are obtained by solving the three-dimensional governing equations namely the following: continuity for conservation of mass, Navier-Stokes equation for conservation of momentum and energy equation. Fluid domain of water and solid domain of micro-channel heat sink are meshed separately and proper interface is defined in ANSYS CFX Pre for capturing the flow physics. The meshing of fluid and solid domains is carried out in ICEMCFD tool using blocking methodology. Only one fluid channel and two solid domains, each half on either side of the fluid domain, are considered in the analysis and the entire model with 122 channels is not simulated. Symmetry boundary condition is applied on either side of the solid domains of the MCHS assembly. Three MCHS models are considered with varying heights of 3 mm, 4.5 mm and 7 mm keeping the other dimen-

Please cite this article in press as: D.R.S. Raghuraman et al., Influence of aspect ratio on the thermal performance of rectangular shaped micro channel heat sink using CFD code, Alexandria Eng. J. (2016), http://dx.doi.org/10.1016/j.aej.2016.08.033

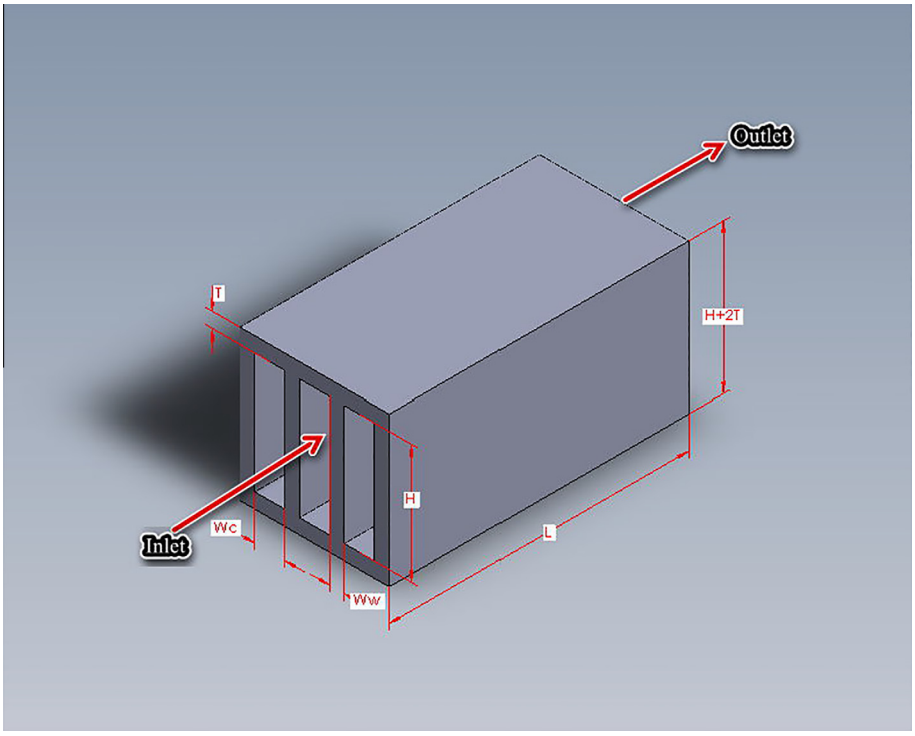

Figure 1 Block diagram of micro channel heat sink assembly.

Table 1 Geometry details of the MCHS.

Micro channel height (H)	7 mm
Micro channel length (L)	31 mm
Base and top thickness (T)	3 mm
Micro channel width (W_w)	150 μm
Micro channel wall width (W_c)	150 μm
Number of micro channels (n)	122

sions namely length and breadth to be constants. The numerically predicted results of 7 mm were validated against the experiments carried out in the laboratory at National Institute of Technology, Trichy. Upon good agreement between the numerically predicted results and experimental data the numerical analysis is extended to MCHS assembly with heights of 3 mm and 4.5 mm keeping the same boundary conditions. The thickness of the channel wall is also maintained at 150 μm for all the three cases. The height of 3 mm, 4.5 mm and 7 mm corresponds to an aspect ratio of 20, 30 and 46.66 respectively for the MCHS considered. The aim behind cre-

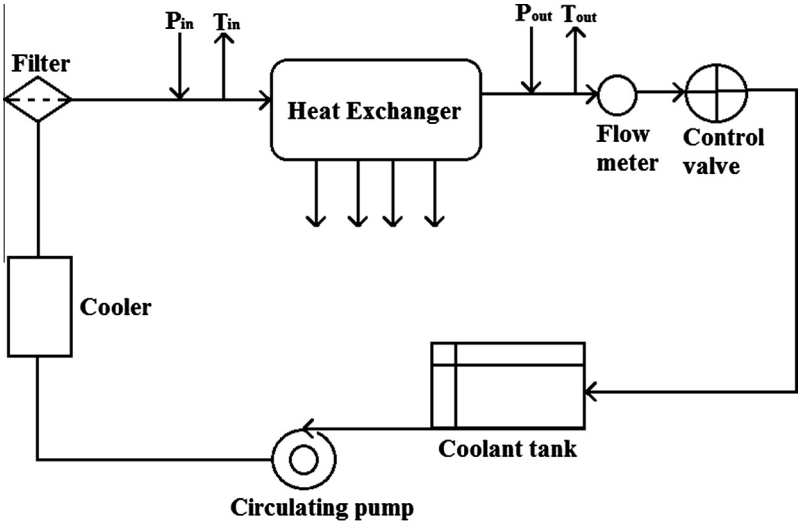

Figure 2 Schematic layout of experimental test setup.

Figure 3 Experimental setup of MCHS with measuring instruments.

ation of additional geometries of the MCHS was to obtain an optimum size of MCHS exhibiting better heat transfer characteristics with minimum pressure drop characteristics.

3.2. Grid generation – finite volume discretization

The three-dimensional discretized model is generated in the meshing tool ICEMCFD in the pre-processor phase as shown in Fig. 4. The entire domain is discretized into finite volume hexahedral elements to capture the thermal and hydraulic boundary layers as shown in Fig. 5 by very fine grids near the walls. A y^+ value of less than 1 is maintained near the fluid solid interface to capture this phenomenon. The minimum angle and determinant of the hexahedral elements are maintained at 90° and 1 respectively, which ensures very good quality of the finite volume discretization. The micro channel has discrete zones as solid and fluid domains. The fluid domain is surrounded by solid copper domain on either side and the

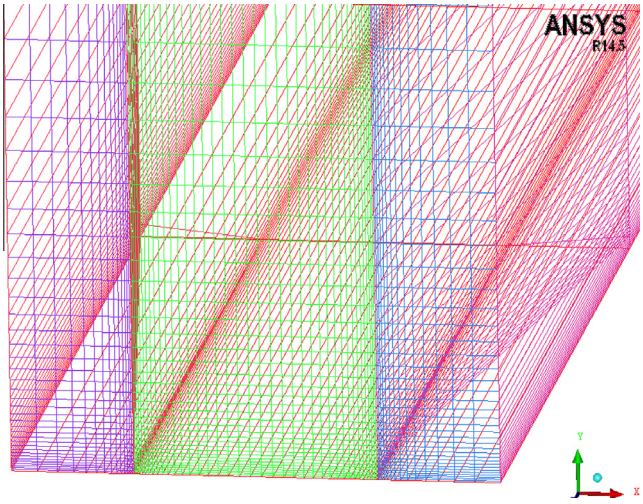

Figure 5 Zoomed view of hexahedral mesh influencing boundary layer growth.

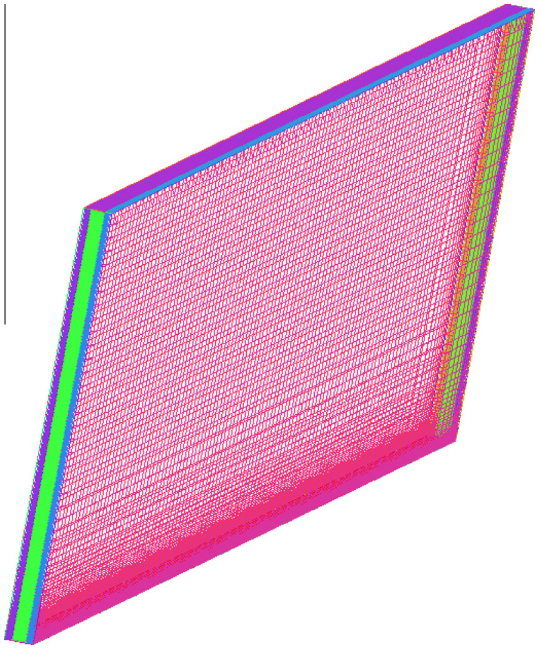

Figure 4 Discretized finite volume hexahedral elements of the MCHS.

corresponding fluid solid interfaces are defined in the pre-processor as shown in Table 2. The inlet boundary is velocity inlet and pressure boundary of zero gauge pressure is applied at the fluid outlet for the exit boundary condition. The interfaces defined enable fluid flow visualization across the MCHS. Since heat transfer through conduction takes place along the copper solid wall, convection between the heated bottom wall surface and the liquid, the meshing is made very fine in order to simulate conjugate heat transfer which is a combination of conductive and convective heat transfers. The heat transfer by radiation is minimal and negligible and hence in this numerical study radiation effects are not considered.

3.3. Governing equations

The governing equations are the standard continuity equation for conservation of mass, Navier – Stokes equation for conservation of momentum and energy equations for predicting the conjugate heat transfer. The following conditions are assumed in this numerical analysis:

(1) Steady fluid flow and heat transfer
(2) Incompressible fluid

Table 2 Boundary conditions and interfaces conceived in the ANSYS-CFX preprocessor.

Sl.no	Solid domain	Fluid domain	Interface/boundary location	Interface/boundary type
1	Copper	Water	FLSO_Left	Fluid Solid
2	Copper	Water	FLSO_Right	Fluid Solid
3	Copper	Water	FLSO_Bottom	Constant Heat Flux
4	Copper	–	Bottom Wall	Constant Heat Flux
5	Copper	Water	FLSO_Top	Adiabatic
6	Copper	–	Top_Wall	Adiabatic
7	–	Water	Fluid_Inlet	Velocity Inlet
8	–	Water	Fluid_Outlet	Pressure Outlet (0 Gauge Pressure)

(3) Laminar flow
(4) Negligible radiative heat transfer
(5) Constant solid and fluid flow properties

The above assumptions are incorporated to derive the governing differential equations for fluid flow and heat transfer as below:

Continuity equation:

$$\nabla \cdot (\rho \vec{V}) = 0 \tag{1}$$

Momentum equation:

$$\nabla \cdot (\rho u \vec{V}) = -\frac{\partial p}{\partial x} + \frac{\partial \tau_{xx}}{\partial x} + \frac{\partial \tau_{yx}}{\partial y} + \frac{\partial \tau_{zx}}{\partial z}$$

$$\nabla \cdot (\rho u \vec{V}) = -\frac{\partial p}{\partial y} + \frac{\partial \tau_{xy}}{\partial x} + \frac{\partial \tau_{yy}}{\partial y} + \frac{\partial \tau_{zy}}{\partial z}$$

$$\nabla \cdot (\rho u \vec{V}) = -\frac{\partial p}{\partial z} + \frac{\partial \tau_{xz}}{\partial x} + \frac{\partial \tau_{yz}}{\partial y} + \frac{\partial \tau_{zz}}{\partial z} \tag{2}$$

Energy equation:

$$\nabla \cdot (\rho e \vec{V}) = -p\nabla \cdot \vec{V} + \nabla \cdot (K\nabla T) + q + \phi \tag{3}$$

The above equations are solved using a segregated solver. The continuity equation and momentum equations are solved in a sequential strategy. Because the governing equations are nonlinear, it requires several iterations in the solution loop to get a converged solution. The Navier-Stokes equations are used to solve the momentum equations which only consider the mean velocity components and the turbulence is not modeled as the flow is laminar in nature through the micro channel heat sinks.

These equations of continuum hold good for the present MCHS model. The second order upwind scheme is used to model the laminar fluid flow with viscous friction. The walls of the MCHS are smooth and no slip boundary conditions are considered at the wall surface. The flow velocity inside the MCHS is very low and hence the laminar flow condition is considered in this numerical analysis.

3.4. Numerical solving

The finite volume method is used to solve the continuity, momentum and energy equations.

In this method, the domain is divided into many control volumes and the integral form of the governing equations is solved using a continuum approach. The governing equations are integrated over the entire control volumes in order to obtain algebraic equations for pressure, temperature and velocities. The convergence for mass and momentum imbalance is targeted less than 10e−06 and 10e−08 for energy imbalance.

3.5. Boundary conditions

The boundary conditions defined in the ANSYS-CFX processor serve as inputs for the model. The flow considered is laminar and the corresponding boundary conditions and interfaces are provided in Table 2.

The fluid used in this numerical analysis is water and its corresponding thermo physical properties are obtained at 33 °C, similar to those of experimental investigations.

1. The inlet water temperature is 33 °C
2. A constant heat flux is assigned to the bottom wall surfaces
3. The inlet is velocity and is assumed uniform
4. No slip boundary condition is assigned to all the surfaces
5. The side and top walls of the MCHS are made insulated
6. Zero gauge pressure is assigned at the outlet of the MCHS

In ANSYS CFX solver, the conservation equations are solved at discretized pseudo time steps and the solutions are obtained based on the convergence of mass, momentum and energy equations. An iterative process is carried out by repeated solving of the governing equations; thereby, the errors converge to a bare minimum value up to five decimal places for mass and momentum and up to 7 decimal places for energy which means theoretically almost zero. Thus the solutions obtained are more reliable with higher values of convergence. The number of elements used for discretizing the domain and the equations selected for fluid flow and conjugate heat transfer greatly influence the quality of the results achieved.

3.6. Post processing and data extraction

The post processing operation is carried out in the ANSYS-CFX software after developing the model, discretizing and solving the governing equations by incorporating the appropriate boundary conditions. The following data are deduced from the post-processor as given below.

3.6.1. Pressure drop and friction factor

The important parameter namely friction factor (f) is calculated based on the formula given below.

$$f = (2 \times \nabla P \times D_h)/(L \times \rho \times u^2 m) \tag{4}$$

The friction factor is obtained by predicting the pressure drop along the length of the micro-channel and is obtained using ANSYS CFX post-processor.

The hydraulic diameter of the MCHS is given by $4A/P$ where A is given by the product of the height and width of the micro-channel ($A = H \times W_c$) and P is given by $2 \times (H + W_c)$. It is found that the friction factor is inversely proportional to the mean square velocity of the fluid flow. As expected the friction factor decreases with increase in Reynolds number in all the numerical simulations considered.

Reynolds number is provided as input for the numerical simulations for three different aspect ratios of micro channel heat sinks. The Reynolds number is varied from 50 to 350 in steps of 50 each corresponding to seven numerical simulations for a particular aspect ratio. The Reynolds number is given by the formula

$$R_e = \rho u_m D_h/\mu \tag{5}$$

3.6.2. Heat transfer characteristics

Temperatures along the length of the micro channel at different points are predicted using CFD tool and are used to find the average wall temperature. The difference in temperature between the outlet and inlet is used to calculate the heat taken away by the water and is given by the following equation:

$$Q = m \times c_p \times (T_{out} - T_{in}) \tag{6}$$

The average wall heat transfer coefficient for the flow through the micro channel heat sink is obtained as follows:

$$h_{avg} = Q/(A_{eff} \times T_{out} - T_{in}) \tag{7}$$

An important non-dimensional number for quantifying heat transfer is estimated by the calculation of Nusselt Number and is given by the equation:

$$N_u = hD_h/k \tag{8}$$

This Nusselt number based on the average heat transfer coefficients gives a better understanding of effective heat transfer from the MCHS to the fluid and it can be compared with various Reynolds number. It is found that the increase in Reynolds number leads to an increase in Nusselt number thereby aiding better heat transfer characteristics.

4. Validation and grid independence study

The result of any numerical simulation is greatly affected by the number of elements used for discretizing the fluid and solid domains. The accuracy of the results obtained increases with increase in number of cell elements used to discretize the domain. The type of cell elements also greatly influences the predicted results, especially in case of flow through domains such as Micro Channel Heat Sinks (MCHS). In this study hexahedral cells are used for capturing the flow physics such as thermal and hydrodynamics boundary layers more accurately. A grid independence study is carried out for MCHS with aspect ratio of 46.66 corresponding to a height of 7 mm and 150 μm width. The solution is obtained for three mesh densities corresponding to 187,900, 312,748 and 454,327 hexahedral elements.

The temperature contours of the predicted results for the above three mesh densities are compared with the experiments carried out in the laboratory. It is found that the numerically predicted results are grid independent beyond 312,748 elements and the deviation between the numerically predicted results and experiments for temperature and pressure drops is well below 5% as shown in Fig. 6. The experiments are carried out on the MCHS with Reynolds number varying from 50 to 350 in steps of 50 and the same has been simulated using CFD for validation purpose. Similar grid independence studies are carried out for MCHS with AR of 30 and 45 for all the Reynolds number considered. Since the deviation between the predicted results and experiments is less than 5% the numerical tool can be extended with confidence to undergo parametric studies with various aspect ratios and mass flow rates.

5. Results and discussion

Numerical studies are carried out for three aspect ratios of 20.00, 30.00 and 46.66 corresponding to the heights of 3, 4.5 and 7 mm respectively of the micro channel heat sink keeping the width constant at 150 μm. For the numerical simulation, the Reynolds number for each case is varied from 50 to 350 in steps of 50 contributing to seven cases for a particular aspect ratio of the micro channel heat sink and hence a total of 21 numerical cases are studied for three aspect ratios of the MCHS as given in the below Table 3.

5.1. Fluid flow characteristics

An attempt has been made to study the fluid flow and heat transfer characteristics of micro channel heat sink with respect to Reynolds number which is non-dimensional in nature. The previous studies in the literature had been carried out with respect to inlet velocity and volumetric flow rate. In this numerical study an attempt is made to optimize the height of the MCHS. The height of the MCHS is reduced to 3 mm and 4.5 mm from its original dimension of 7 mm and the results with respect to the fluid flow and heat transfer characteristics are presented.

In this study, the pressure drop profiles of micro channel heat sinks (MCHS) with three aspect ratios of 20.00, 30.00

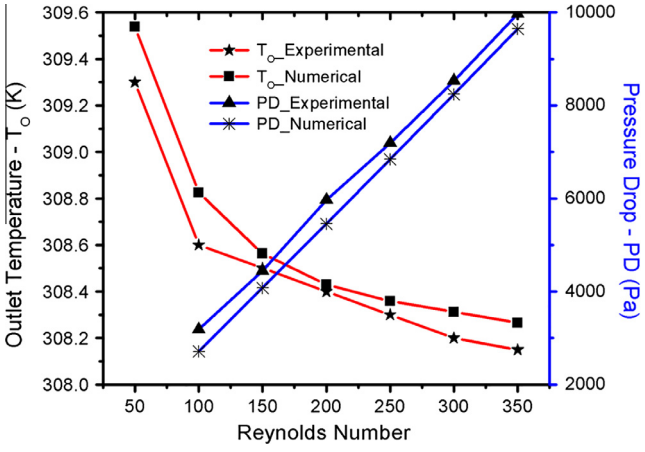

Figure 6 Outlet temperature and pressure drop vs R_e for MCHS with AR of 46.66.

Table 3 List of numerical cases.

S. no	Aspect ratio	Reynolds number	Height of the MCHS (mm)
Case 1	20.00	50	3
Case 2	20.00	100	3
Case 3	20.00	150	3
Case 4	20.00	200	3
Case 5	20.00	250	3
Case 6	20.00	300	3
Case 7	20.00	350	3
Case 8	30.00	50	4.5
Case 9	30.00	100	4.5
Case 10	30.00	150	4.5
Case 11	30.00	200	4.5
Case 12	30.00	250	4.5
Case 13	30.00	300	4.5
Case 14	30.00	350	4.5
Case 15	46.66	50	7
Case 16	46.66	100	7
Case 17	46.66	150	7
Case 18	46.66	200	7
Case 19	46.66	250	7
Case 20	46.66	300	7
Case 21	46.66	350	7

and 46.66 are plotted against Reynolds number ranging from 50 to 350 in steps of 50. It is found that the pressure drop increases as the Reynolds number increased as expected for all the three different types of micro channel heat sinks as shown in Fig. 7. The pressure drop increases with increase in Reynolds number as the mass flow rate increases. It is found from Fig. 7 that the pressure drop of MCHS with AR 20 is greater than the MCHS with AR of 30 and 46.66 even though the maximum mass flow is 361 mg/s for MCHS with AR 20 and the corresponding maximum mass flow rate is 819 mg/s for AR of 46.66. This is because the area of MCHS with AR 46.66 is more compared to the areas of other two types of MCHS. Thus it is found that the pressure drop is not only dependent on the mass flow rate but also depends on the available cross-sectional area. It is also found that the maximum flow rate is obtained for MCHS with AR 46.66 compared to the other two types of MCHS as shown in Fig. 8 for the same Reynolds number.

The friction factor for all three types of MCHS has almost the same value and a slight deviation exists between them as seen in Fig. 7. The friction factor of MCHS with AR 46.66 is slightly higher than that of other two types of MCHS but the variation is also negligible. Thus it is found that even though the pressure drop of MCHS with AR 20 is higher, the friction factor remains almost the same. This is because the friction factor as described in Eq. (5) not only depends on pressure drop, but also with hydraulic diameter and square of the inlet velocity.

Pumping power (W_{PP}) is defined as the amount of energy required to pump the water from inlet to outlet of the micro channel per unit time. It is defined as follows:

$$W_{pp} = n \cdot V \cdot \nabla P \tag{9}$$

Fig. 8 shows that the pumping power increases with increases in mass flow rate through the MCHS. Pumping power is a parameter which depends on the volumetric flow rate and

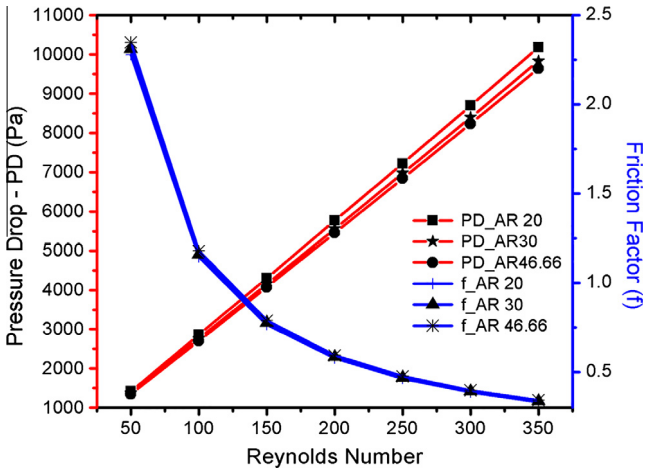

Figure 7 Pressure drop and friction factor vs R_e for MCHS with varying aspect ratio.

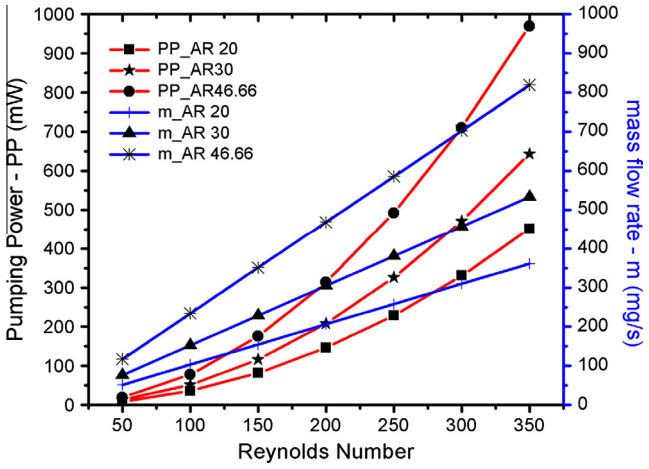

Figure 8 Pumping power and mass flow rate vs R_e for MCHS with varying aspect ratio.

the pressure drop across the channel as given in the above equation. It is to be noted that even though the pressure drop for AR 20 is higher the pumping power of AR 20 is lesser due to very low mass flow rate compared to the other two types of MCHS. The mass flow rate through AR 46.66 is nearly 3 times greater than that of AR 20 MCHS as seen in Fig. 8. Thus from this numerical analysis, it is found that the flow rate plays a dominant role in determining the pumping power compared to the pressured drop for the numerical cases investigated. It is to be noted at this juncture, the pumping power is calculated for all the 122 channels of the MCHS and the plot drawn for the mass flow rate is based on a single channel of the MCHS. The pumping power of MCHS with AR 30 is in between MCHS with AR 20 and AR 46.66 and moreover the gradient between AR 30 and AR 20 is lesser compared to MCHS with AR of 46.66 and 30.

5.2. Heat transfer characteristics

The variation of temperature at outlet of the MCHS is shown in Fig. 9. It is found that the outlet temperature (T_o) of MCHS

with AR 46.66 is lesser than other two types of MCHS. The reasons are twofold: (i) The mass flow rate through MCHS with AR 46.66 is more with the same heat input at the bottom surface and (ii) the height of the MCHS is long and hence the fluid particles moving at the top layer cannot get the heat input from the base as compared to the fluid elements nearer to the bottom surface. The outlet temperatures of MCHS with AR 20 and AR 30 are almost the same and the values of AR 40 are slightly lesser than those of AR 20 and the above two reasons hold good here too. A similar trend is obtained for the maximum wall temperature (T_W) which is obtained at the base surface where heat is to be removed as shown in Fig. 9. It is seen for all the numerical cases investigated the outlet temperature and maximum wall temperature decreases with increases in Reynolds number and the gradient being steep at the earlier stage compared to the later stage.

A plot of Nusselt number (N_u) vs Reynolds number (R_e) for MCHS with various ARs is shown in Fig. 10. It is found that the Nusselt number of MCHS with AR 20 has higher Nusselt compared to MCHS of AR 30 and 46.66. It is also seen that Nusselt number increases with increase in Reynolds number for all the numerical cases investigated. Lesser Nusselt number of MCHS with AR 46.66 indicates relatively poorer convective heat transfer from the base surface to the fluid and this is because of increased height of the channel. The Nusselt number of AR 30 MCHS is slightly lower than that of AR 20 for the Reynolds number analyzed.

The main objective in designing of any MCHS was to remove the maximum heat with optimal pressure drop so that the pumping power would be minimal. The total heat removed in case of MCHS with AR 46.66 is lesser compared to other two types of MCHS with AR 20 and AR 30, because of lesser N_u which indicates poorer convective heat transfer and is quite obvious as reflected in Fig. 10. With the same approach, the heat removed by MCHS of AR 20 should be higher than AR 30. But the results are reverse due to the fact that the mass flow rate of MCHS with AR 30 is more than AR 20 for the same Reynolds number as given in Eq. (7). Even though the pumping power of AR 20 is slightly lower than AR 30, MCHS with AR 30 is preferred since it is able to remove 16% more heat from the source than MCHS with AR 20.

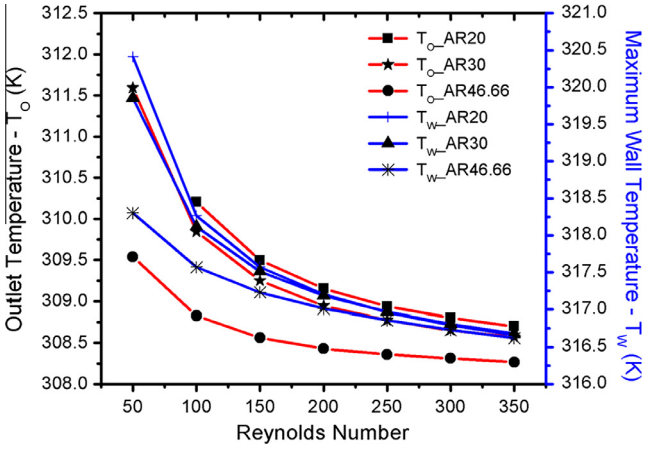

Figure 9 Outlet and maximum wall temperature vs R_e for MCHS with varying aspect ratio.

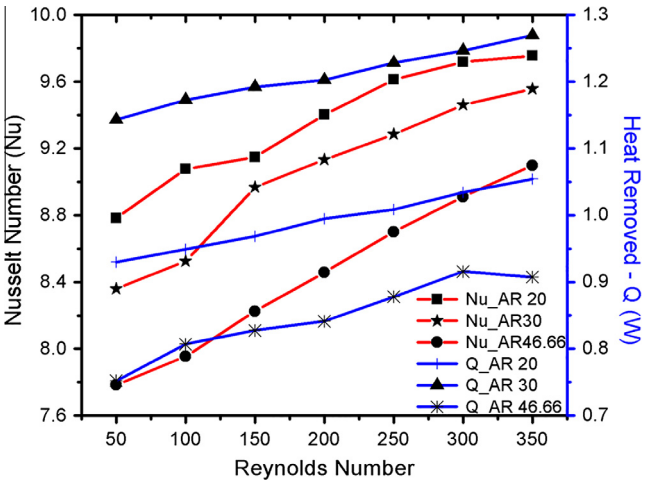

Figure 10 N_u and heat removed vs R_e for MCHS with varying aspect ratio.

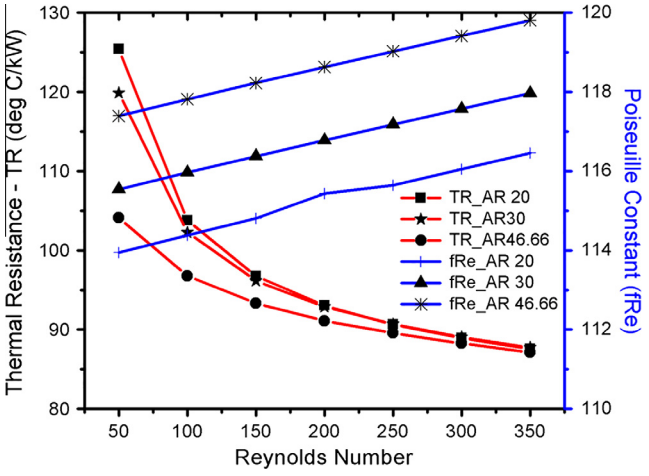

Figure 11 Thermal resistance and Poiseuille constant vs R_e for MCHS with various ARs.

Thermal Resistance is the property which defines the resistance to heat flow from the base source to the working fluid. It is defined as follows:

$$\text{Thermal Resistance (TR)} = (T_{Wmax} - T_{in})/Q_b \quad (10)$$

It is seen from Fig. 11 that the thermal resistance decreases with increase in Reynolds number due to increase in Nusselt number for all the cases considered. It is found that the thermal resistance of MCHS with AR 20 is higher compared to the other two types of MCHS with AR 30 and 46.66. The heat removed by AR 20 is lesser and this may be due to high thermal resistance as shown in Fig. 11. The variation in thermal resistance for MCHS is higher at low Reynolds number and approaches same value at a Reynolds number of 350.

Poiseuille Constant (P_c) is defined as the product of friction factor (f) and the Reynolds number (R_e). It is well known that the friction factor decreases with increases in Reynolds number and hence better heat transfer characteristics due to better convection. But when the Reynolds number increases the pumping

Please cite this article in press as: D.R.S. Raghuraman et al., Influence of aspect ratio on the thermal performance of rectangular shaped micro channel heat sink using CFD code, Alexandria Eng. J. (2016), http://dx.doi.org/10.1016/j.aej.2016.08.033

power also increases due to more mass flow rate and hence a need of plotting Poiseuille constant (P_c) with Reynolds number is necessary. It is found from Fig. 11 that P_c increases with increase in Reynolds number for all the cases considered. It is found that P_c for AR 46.66 is higher than AR 30 which in turn is higher than AR20. The product of fR_e should remain a constant for laminar flow in conventional size but it increases with increase in Reynolds number due to the size of the micro channel and its variation may also due to constant velocity profile at the inlet as quoted by Xie et al. [21].

6. Conclusions

1. The pressure drop of MCHS with AR 20 is higher than MCHS with AR 30 and 46.66, whereas the pumping power of MCHS with AR 46.66 is higher because of more mass flow rate transferred along the length of the micro channel.
2. The mass flow rate through MCHS with AR 46.66 is higher for the same Reynolds number considered and hence the average outlet temperature of the fluid is lesser for MCHS with AR 46.66 compared to the MCHS with AR 30 and AR 20.
3. Thermal Resistance of AR 20 is higher than the other two types of MCHS and the Poiseuille's constant also linearly increases with Reynolds number for all the different types of MCHS.
4. Even though the Nusselt number of MCHS with AR 20 is higher than the other two types of MCHS with AR 30 and AR 46.66, it is found that MCHS with AR 30 has higher heat removal rate as compared to the other two types of MCHS.
5. Considering the various operating parameters such as pressure drop, friction factor, Nusselt number, thermal resistance, Poiseuille's constant and pumping power the MCHS with AR 30 is preferred since it could remove more amount of heat keeping the other parameters at optimum level from the numerical cases investigated.

References

[1] D.B. Tuckerman, R.F. Pease, High-performance heat sinking for VLSI, IEEE Electr. Device Lett. 2 (5) (1981) 126–129.
[2] M.E. Steinke, S.G. Kandlikar, Single-phase liquid friction factors in microchannels, ASME 3rd International Conference on Microchannels and Minichannels, vol. 1, American Society of Mechanical Engineers, 2005, pp. 291–302.
[3] R. Rathanasamy, K. Kalaivanan, Experimental investigation of forced convective heat transfer in rectangular micro-channels, ARPN J. Eng. Appl. Sci. 5 (5) (2010) 21–26.
[4] M. Iyengar, S. Garimella, Design and optimization of microchannel cooling systems, Thermal and Thermomechanical Phenomena in Electronics Systems, 2006. ITHERM'06. The Tenth Intersociety Conference on 2006 May 30, IEEE, 2006, pp. 54–62.
[5] W.H. Wong, N.M. Ghazali, Numerical simulation of a microchannel for microelectronic cooling, J. Teknologi 46 (1) (2012) 1–6.
[6] M.J. Ellsworth, L.A. Campbell, R.E. Simons, R.R. Iyengar, The evolution of water cooling for IBM large server systems: back to the future, in: Thermal and Thermomechanical Phenomena in Electronic Systems, 2008. ITHERM 2008. 11th Intersociety Conference on 2008 May 28, IEEE, 2008, pp. 266–274.
[7] W. Qu, G.M. Mala, D. Li, Heat transfer for water flow in trapezoidal silicon microchannels, Int. J. Heat Mass Transf. 43 (21) (2000) 3925–3936.
[8] P. Naphon, O. Khonseur, Study on the convective heat transfer and pressure drop in the micro-channel heat sink, Int. Commun. Heat Mass Transf. 36 (1) (2009) 39–44.
[9] S. Yu, T.A. Ameel, Slip-flow heat transfer in rectangular microchannels, Int. J. Heat Mass Transf. 44 (22) (2001) 4225–4234.
[10] M.J. Khan, M.R. Hasan, M.A. Mamun, Flow behavior and temperature distribution in micro-channels for constant wall heat flux, Procedia Eng. 56 (2013) 350–356.
[11] P.M. Khameneh, I. Mirzaie, N. Pourmahmoud, M. Rahimi, S. Majidyfar, A numerical study of single-phase forced convective heat transfer in tube in tube heat exchangers, World Acad. Sci. Eng. Technol. Int. J. Mech. Aerospace Ind. Mechatronic Manuf. Eng. 4 (10) (2010) 958–963.
[12] D.R. Raghuraman, P.K. Nagarajan, S. Suresh, Thermal performance of higher aspect ratio microchannels using TiO_2-water nanofluids, J. Nanosci. Nanotechnol. 13 (4) (2013) 2842–2846.
[13] N.I. Amanifard, A.K. Haghi, Numerical analysis of fluid flow and heat transfer in microchannels, Int. J. Heat Technol. 25 (1) (2007) 103–110.
[14] W. Qu, I. Mudawar, Experimental and numerical study of pressure drop and heat transfer in a single-phase micro-channel heat sink, Int. J. Heat Mass Transf. 45 (12) (2002) 2549–2565.
[15] Y. Mishan, A. Mosyak, E. Pogrebnyak, G. Hetsroni, Effect of developing flow and thermal regime on momentum and heat transfer in micro-scale heat sink, Int. J. Heat Mass Transf. 50 (15) (2007) 3100–3114.
[16] I. Hassan, P. Phutthavong, M. Abdelgawad, Microchannel heat sinks: an overview of the state-of-the-art, Microscale Thermophys. Eng. 8 (3) (2004) 183–205.
[17] P. Selvaraj, J. Sarangan, S. Suresh, Computational fluid dynamics analysis on heat transfer and friction factor characteristics of a turbulent flow for internally grooved tubes, Therm. Sci. 17 (4) (2013) 1125–1137.
[18] R. Zhang, M. Hodes, N. Lower, R. Wilcoxon, High heat flux, single-phase microchannel and minichannel cooling with water and liquid metal, Electron. Cooling (2014).
[19] M.R. Salimpour, M. Sharifhasan, E. Shirani, Constructal optimization of microchannel heat sinks with noncircular cross sections, Heat Transf. Eng. 34 (10) (2013) 863–874.
[20] V.V. Dharaiya, S.G. Kandlikar, Numerical investigation of heat transfer in rectangular microchannels under H_2 boundary condition during developing and fully developed laminar flow, J. Heat Transf. 134 (2) (2012) 020911.
[21] X.L. Xie, Z.J. Liu, Y.L. He, W.Q. Tao, Numerical study of laminar heat transfer and pressure drop characteristics in a water-cooled minichannel heat sink, Appl. Therm. Eng. 29 (1) (2009) 64–74.
[22] G. Xie, F. Zhang, B. Sundén, W. Zhang, Constructal design and thermal analysis of microchannel heat sinks with multistage bifurcations in single-phase liquid flow, Appl. Therm. Eng. 62 (2) (2014) 791–802.
[23] T.C. Hung, Y.X. Huang, W.M. Yan, Thermal performance analysis of porous-microchannel heat sinks with different configuration designs, Int. J. Heat Mass Transf. 66 (2013) 235–243.
[24] L. Lin, Y.Y. Chen, X.X. Zhang, X.D. Wang, Optimization of geometry and flow rate distribution for double-layer microchannel heat sink, Int. J. Therm. Sci. 78 (2014) 158–168.
[25] G. Xie, Y. Li, F. Zhang, B. Sundén, Analysis of micro-channel heat sinks with rectangular-shaped flow obstructions, Numer. Heat Transf. Part A: Appl. 69 (4) (2016) 335–351.
[26] M. Sheikholeslami, M.G. Bandpy, R. Ellahi, A. Zeeshan, Simulation of MHD CuO–water nanofluid flow and

convective heat transfer considering Lorentz forces, J. Magn. Magn. Mater. 369 (2014) 69–80.
[27] A. Zeeshan, R. Ellahi, M. Hassan, Magnetohydrodynamic flow of water/ethylene glycol based nanofluids with natural convection through a porous medium, Eur. Phys. J. Plus 129 (12) (2014) 1.
[28] A. Zeeshan, A. Majeed, Non Darcy mixed convection flow of magnetic fluid over a permeable stretching sheet with ohmic dissipation, J. Magn. 21 (1) (2016) 153–158.
[29] A. Zeeshan, A. Majeed, R. Ellahi, Effect of magnetic dipole on viscous ferro-fluid past a stretching surface with thermal radiation, J. Mol. Liq. 215 (2016) 549–554.
[30] R. Ellahi, M. Hassan, A. Zeeshan, Shape effects of nanosize particles in Cu–H_2O nanofluid on entropy generation, Int. J. Heat Mass Transf. 81 (2015) 449–456.

Please cite this article in press as: D.R.S. Raghuraman et al., Influence of aspect ratio on the thermal performance of rectangular shaped micro channel heat sink using CFD code, Alexandria Eng. J. (2016), http://dx.doi.org/10.1016/j.aej.2016.08.033